Identification of (-)-bornyl diphosphate synthase from *Blumea balsamifera* and its application for (-)-borneol biosynthesis in *Saccharomyces cerevisiae*

Rui Ma [a,b,1], Ping Su [b,1], Qing Ma [b,1], Juan Guo [b], Suiqing Chen [a], Baolong Jin [b], Haiyan Zhang [b], Jinfu Tang [b], Tao Zhou [c], Chenghong Xiao [c], Guanghong Cui [b,*], Luqi Huang [a,b,**]

[a] *School of Pharmacy, Henan University of Chinese Medicine, Zhengzhou, China*
[b] *State Key Laboratory Breeding Base of Dao-di Herbs, National Resource Center for Chinese Materia Medica, China Academy of Chinese Medical Sciences, Beijing, China*
[c] *School of Pharmacy, Guizhou University of Traditional Chinese Medicine, Guiyang, China*

ARTICLE INFO

ABSTRACT

Borneol is a precious monoterpenoid with two chiral structures, (-)-borneol and (+)-borneol. Bornyl diphosphate synthase is the key enzyme in the borneol biosynthesis pathway. Many (+)-bornyl diphosphate synthases have been reported, but no (-)-bornyl diphosphate synthases have been identified. *Blumea balsamifera* leaves are rich in borneol, almost all of which is (-)-borneol. In this study, we identified a high-efficiency (-)-bornyl diphosphate synthase (BbTPS3) from *B. balsamifera* that converts geranyl diphosphate (GPP) to (-)-bornyl diphosphate, which is then converted to (-)-borneol after dephosphorylation *in vitro*. BbTPS3 exhibited a K_m value of 4.93 ± 1.38 μM for GPP, and the corresponding k_{cat} value was 1.49 s^{-1}. Multiple strategies were applied to obtain a high-yielding (-)-borneol producing yeast strain. A codon-optimized BbTPS3 protein was introduced into the GPP high-yield strain MD, and the resulting MD-B1 strain produced 1.24 mg·L^{-1} (-)-borneol. After truncating the N-terminus of BbTPS3 and adding a Kozak sequence, the (-)-borneol yield was further improved by 4-fold to 4.87 mg·L^{-1}. Moreover, the (-)-borneol yield was improved by expressing the fusion protein module of ERG20$^{F96W-N127W}$-YRSQI-t14-BbTPS3K2, resulting in a final yield of 12.68 mg·L^{-1} in shake flasks and 148.59 mg·L^{-1} in a 5-L bioreactor. This work is the first reported attempt to produce (-)-borneol by microbial fermentation.

1. Introduction

(-)-Borneol, a bicyclic monoterpene alcohol that is present in the essential oils of *Blumea balsamifera* (L.) DC., is widely used in the perfumery, cosmetics, and pharmaceutical industries [1,2]. It has been used medicinally for centuries in China for the treatment of stroke, and it is also used as a messenger drug to facilitate the transport of multiple drugs to specific sites by increasing blood-brain barrier permeability [3–5]. In addition, (-)-borneol and its derivatives exhibit a wide range of medicinal properties, such as anti-inflammatory, antimicrobial, and antiviral activities [6,7]. (-)-Borneol is mainly obtained from the fresh leaves of the plant *B. balsamifera* through distillation. However, the current production levels are not sustainable and cannot meet the increasing global

market demand. As a result, synthetic borneol, which contains a few toxic compounds (e.g., isoborneol), is used widely as an alternative [8].

Recently, the use of emerging synthetic biology platforms has proved to be a promising alternative for monoterpenoid production; sustainable and reliable means of production can be established via engineering the biosynthetic pathways in microbes. Successful examples include the production of geraniol, limonene, linalool, (+)-borneol, citronellol, and nerol. Efforts to improve the efficiency of monoterpene production mainly focus on: (1) improving the geranyl diphosphate (GPP) pool by overexpressing the upstream pathway genes; (2) selecting for monoterpene synthases with higher activity and the same catalytic function; (3) improving the expression level or catalytic activities of monoterpene synthases by truncating the N-terminal transit peptide; and (4) constructing genetic fusions to bring enzymes together for the catalysis of a

Abbreviations

MVA	mevalonate pathway
MEP	2-C-methyl-D-erythritol-4-phosphate pathway
GPP	geranyl diphosphate
BPPS	bornyl diphosphate synthase
ORF	open reading frame
SDS-PAGE	sodium dodecyl sulfate polyacrylamide gel electrophoresis
CIAP	calf intestinal alkaline phosphatase
GC-MS	gas chromatography coupled with mass spectrometry
SD-Leu-Ura	synthetic drop-out medium without leucine and uracil
DO	dissolved oxygen

cascade of reactions [9–13]. It is highly possible that high-titer production of (-)-borneol could be achieved by integrating these strategies to maximize flux toward target products.

(-)-Borneol is mainly derived from GPP, which is synthesized from two common C$_5$ building blocks, isopentenyl diphosphate and dimethylallyl diphosphate, via either the cytoplasmic mevalonate (MVA) or the plastidic 2-C-methyl-D-erythritol-4-phosphate (MEP) pathway [14]. However, the specific monoterpene synthase responsible for cyclization of GPP to form (-)-bornyl diphosphate remains enigmatic, although many (+)-bornyl diphosphate synthases have been reported in plants (e. g., *Cinnamomum burmanni, Salvia officinalis, Amomum villosum, Lippia dulcis,* and *Lavandula angustifolia*) [10,15–18]. Thus, no work has reported the *de novo* synthesis of (-)-borneol in microbes to date.

In this study, we identified a high-specificity (-)-bornyl diphosphate synthase, BbTPS3, from *B. balsamifera*, which is the first monoterpene synthase reported to catalyze the cyclization of GPP forming (-)-bornyl diphosphate, and then dephosphorylated to (-)-borneol by phosphatases. Among the products obtained using GPP as a substrate in an *in vitro* assay, (-)-borneol accounted for 95.30% of the total products. We thus aimed to reconstruct the (-)-borneol biosynthesis pathway and then enhance its production in *Saccharomyces cerevisiae* using multiple strategies. The final strain expressing a fusion module, ERG20$^{F96W-N127W}$-YRSQI-t14-BbTPS3K2, reached a (-)-borneol titer of 148.59 mg·L^{-1} in a 5-L bioreactor. Our research highlights the great opportunity for monoterpene production in microbial cell factories.

2. Materials and methods

2.1. Plant materials and chemicals

Mature and fresh leaves of *Blumea balsamifera* (L.) DC. were obtained from Guizhou Province, China, and identified by Prof. Tao Zhou from Guizhou University of Traditional Chinese Medicine, then stored at −80 °C for further usage (Storage Number: ANX201811). GPP, (+)-borneol and (-)-borneol standards were purchased from Sigma-Aldrich Chemical Co., USA.

2.2. Extraction of borneol in leaves of B. balsamifera

The leaves (n = 6) were ground into powder with a ball mill, aliquots of 80 mg were suspended in 1 mL of ethyl acetate, and then subjected to sonication in an ultrasonic water bath for 60 min. After centrifuging at 13,000×*g* for 10 min, the supernatant was filtered through a 0.22-μm membrane filter (polytetrafluoroethylene) before GC-MS analysis (described below). The calibration curves for content determination are shown in Supplemental Fig. S1.

2.3. RNA extraction and transcriptome sequencing

The total RNA was extracted from *B. balsamifera* leaves using a quick RNA isolation kit (HuaYueYang Biotechnology, China) following the protocol, then submitted to the Illumina sequencing according to the standard process [19]. In brief, 2 μg qualified RNA samples from three biological replicates were mixed and sent to Majorbio (Shanghai, China) to construct a cDNA library on an Illumina Hiseq X Ten (Illumina Inc., San Diego, CA, USA). The Illumina-derived nucleotide sequences reported in this paper have been submitted to China National Center for Bioinformation (https://bigd.big.ac.cn/) under accession number CRA005113.

2.4. BPPS candidate selection and analysis

TBLASTN analysis was used to mine the BPPS candidate genes using BioEdit software [20]. The *CbTPS1* (GenBank Accession Number: MW196671), *LaBPPS* (GenBank Accession Number: AJW68082), *SBS* (GenBank Accession Number: AAC26017), *LdBPPS* (GenBank Accession Number: ATY48638), and *AvBPPS* (GenBank Accession Number: AWW87313) were used as the query sequences. The *BbTPS3* (GenBank Accession Number: OK137535) sequence was analyzed using NCBI (http://www.ncbi.nlm.nih.gov/). The open reading frames (ORFs) were identified using the ORF Finder (http://www.ncbi.nlm.nih.gov/gorf/gorf.html), and deduced amino acid sequences were identified using ExPASy (http://web.expasy.org/translate/). Multiple sequence alignments were conducted using CLC Bio Sequence Viewer 6 (http://www.clcbio.com). The chloroplast transit peptide of CbTPS1 was predicted by ChloroP (http://www.cbs.dtu.dk/services/ChloroP/).

All statistical analyses were conducted using SPSS version 23.0 (SPSS Inc., Chicago, IL, USA) for windows. One-way analysis of variance was used to compare the mean difference in (-)-borneol of strains. The *P*-value of less than 0.05 considered statistically significant.

2.5. Gene cloning, in vitro enzyme assays and kinetic assays

The ORF of candidate gene was cloned using Phusion High-Fidelity PCR Master Mix (New England BioLabs, USA) with the specially designed primers (Supplemental Table 1). The PCR products were purified, and then ligated into the pEASY®-Blunt Simple Cloning Vector (TransGen Biotech, China) and transformed into *E. coli* DH5α cells. Verified the positive colonies by sequencing (Beijing RuiBo Biotechnology Co. Ltd., China) and then subcloned into the pET-32a (+) expression vector (Novagen, USA) according to the protocol of the pEASY®-Uni Seamless Cloning and Assembly Kit (TransGen Biotech, China) (Supplemental Table 1). Recombinant proteins were expressed and purified following the methods described previously [21], and the protein samples were assessed by sodium dodecyl sulfate polyacrylamide gel electrophoresis (SDS-PAGE).

In vitro enzyme assays followed the method described previously [21]. Time-course experiments were carried out to obtain the initial speed of the enzymatic reaction from 3 to 30 min (Fig. S2). Then, 3 min was used in the kinetic assays. The GraphPad Prism version 5 (GraphPad Software, La Jolla California USA, http://www.graphpad.com) was used to obtain kinetic parameters by fitting the obtained data to the Michaelis-Menten equation. All assays were performed in triplicate.

2.6. Construction of (-)-borneol producing strains

The initial strain used in this study was MD (*MATα, URA3-52, TRP1-289, LEU2-3112, HIS3Δ1, MAL2-8C, SUC2, YPRC△15 URA3-P$_{GAL1}$-ERG10-T$_{TPI1}$-P$_{GAL10}$-ERG13-T$_{PGI}$-P$_{GAL1}$-tHMG1-T$_{ADH1}$-P$_{GAL10}$-tHMG1-T$_{CYC1}$-P$_{GAL1}$-tHMG1-T$_{FBA1}$-P$_{GAL10}$-ERG12-T$_{PDC1}$-P$_{GAL1}$-ERG8-T$_{RPS2}$-P$_{GAL10}$-ERG19-T$_{TDH1}$-P$_{GAL1}$-IDI1-T$_{CCW12}$-P$_{GAL10}$-ERG20$^{F96W-N127W}$-T$_{RPL9A}$*, a schematic of strain construction is shown in Fig. S3), which is ultimately derived from *S. cerevisiae* CEN.PK2-1D [10].

Table 1
Information of strains and vectors used in this study.

Strains or Vectors	Description	Source
CEN.PK2-1D	MATα, URA3-52, TRP1-289, LEU2-3112, HIS3Δ1, MAL2-8C, SUC2	EUROSCARF
MD	CEN.PK2-1D, YPRC△15 URA3-P_{GAL1}-ERG10-T_{TPI1}-P_{GAL10}-ERG13-T_{PGI}-P_{GAL1}-tHMG1-T_{ADH1}-P_{GAL10}-tHMG1-T_{CYC1}-P_{GAL1}-tHMG1-T_{FBA1}-P_{GAL10}-ERG12-T_{PDC1}-P_{GAL1}-ERG8-T_{RPS2}-P_{GAL10}-ERG19-T_{TDH1}-P_{GAL1}-IDI1-T_{CCW12}-P_{GAL10}-ERG20$^{F96W/N127W}$-T_{RPL9A}	This study
MD-B1	MD, pESC-LEU::BbTPS3	This study
MD-B2	MD, pESC-LEU::BbTPS3K	This study
MD-B3	MD, pESC-LEU::t14-BbTPS3	This study
MD-B4	MD, pESC-LEU::t14-BbTPS3K	This study
MD-B5	MD, pESC-LEU::t18-BbTPS3	This study
MD-B6	MD, pESC-LEU::t18-BbTPS3K	This study
MD-B7	MD, pESC-LEU::t38-BbTPS3	This study
MD-B8	MD, pESC-LEU::t38-BbTPS3K	This study
MD-B9	MD, pESC-LEU::t14-BbTPS3K2	This study
MD-B10	MD, pESC-LEU::ERG20$^{F96W-N127W}$-GGGS-t14-BbTPS3K2	This study
MD-B11	MD, pESC-LEU::ERG20$^{F96W-N127W}$-GSG-t14-BbTPS3K2	This study
MD-B12	MD, pESC-LEU::ERG20$^{F96W-N127W}$-YRSQI-t14-BbTPS3K2	This study
MD-B13	MD, pESC-LEU::ERG20$^{F96W-N127W}$-VIPFIS-t14-BbTPS3K2	This study
MD-B14	MD, pESC-LEU::ERG20$^{F96W-N127W}$-WRFSPKLQ-t14-BbTPS3K2	This study
MD-B15	MD, pESC-LEU::ERG20$^{F96W-N127W}$-GGGS-t14-BbTPS3K2-2	This study
MD-B16	MD, pESC-LEU::t14-BbTPS3K2-GGGS-ERG20$^{F96W-N127W}$-2	This study

For (-)-borneol production, the yeast codon-optimized BbTPS3 as well as three truncated variants of BbTPS3 (at positions T14, I18 and T38) were cloned into the *BamH*I site of the pESC-Leu vector (Agilent Technologies, USA) according to the pEASY-Uni Seamless Cloning and Assembly Kit (TransGen Biotech, Beijing, China), yielding the plasmids pESC-Leu:*BbTPS3*, pESC-LEU:*t14-BbTPS3*, pESC-LEU:*t18-BbTPS3*, and pESC-LEU:*t38-BbTPS3*. Kozak sequence "GCCACC" was added in front of the START codon ATG of BbTPS3 and the three truncated variants, generating pESC-LEU:*BbTPS3K*, pESC-LEU:*t14-BbTPS3K*, pESC-LEU:*t18-BbTPS3K*, and pESC-LEU:*t38-BbTPS3K*. Further, yeast-specific Kozak sequence "AAAAAA" was added in front of the START codon ATG of pESC-LEU:*t14-BbTPS3*, yielding the plasmid pESC-LEU:*t14-BbTPS3K2* [22–24]. Plasmids with the correct sequence were transferred to the host strain MD using Frozen-EZ Yeast Transformation II™ (Zymo Research, USA) to obtain the (-)-borneol producing strains (Table 1).

The fusion-protein expression plasmids were constructed using the same method. The ERG20$^{F96W-N127W}$ and t14-BbTPS3K2 were coupled together via the flexible linker "GGGS", "GSG", "YRSQI", "VIPFIS", and "WRFSPKLQ". Seven truncated variants of fusion protein were generated (ERG20$^{F96W-N127W}$-GGGS-t14-BbTPS3K2, ERG20$^{F96W-N127W}$-GSG-t14-BbTPS3K2, ERG20$^{F96W-N127W}$-YRSQI-t14-BbTPS3K2, ERG20$^{F96W-N127W}$-VIPFIS-t14-BbTPS3K2, ERG20$^{F96W-N127W}$-WRFSPKLQ-t14-BbTPS3K2, ERG20$^{F96W-N127W}$-GGGS-t14-BbTPS3K2-2, and t14-BbTPS3K2-GGGS-ERG20$^{F96W-N127W}$-2). All the primers used are listed in Supplemental Table 1.

2.7. Shake flask fermentation

For (-)-borneol production, the positive strains were picked into flasks (50 mL) containing 10 mL of synthetic drop-out medium without leucine and uracil (SD-Leu-Ura) (FunGenome, China) at 30 °C and 200 rpm for 48 h. Next, the cells were collected and induced by GAL promoters in 10 mL of YPL (1% yeast extract, 2% peptone, and 2% galactose) medium at 30 °C and 200 rpm for 48 h. The fermentation products were extracted with an equal volume of ethyl acetate for 1 h, and
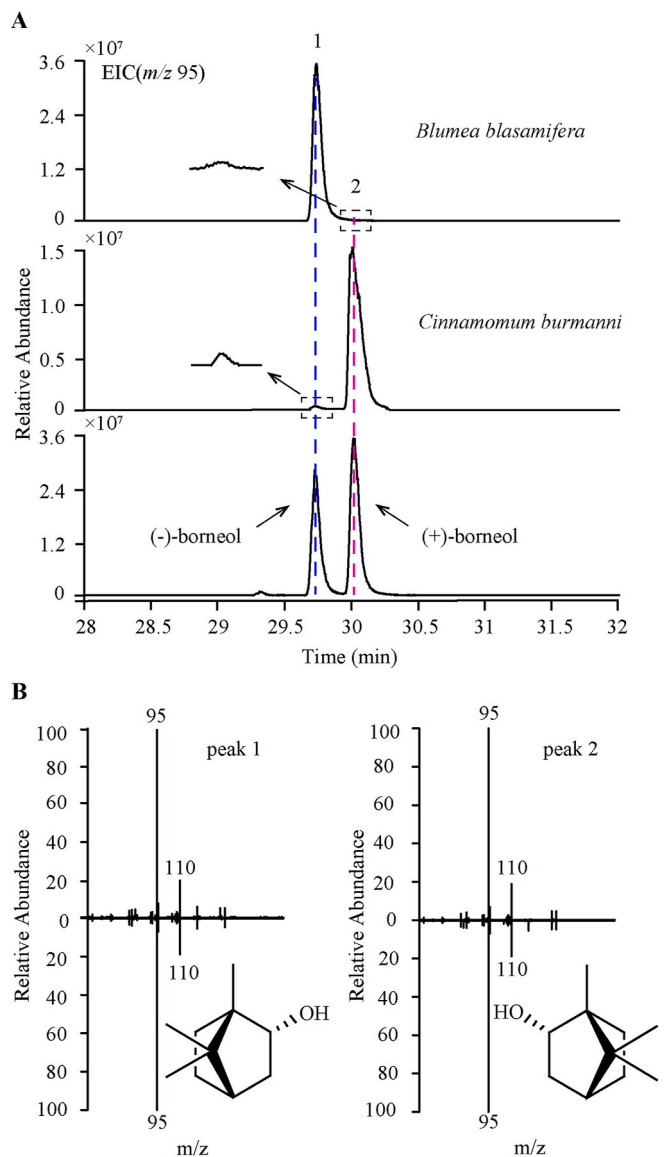
Fig. 1. GC-MS analysis of (−)- and (+)-borneol in *Blumea balsamifera* and *Cinnamomum burmanni* leaves. Extracted ion chromatograms of *m/z* 95 of *B. balsamifera* and *C. burmanni* leaves. (A) Chromatogram of (−)- and (+)-borneol in *B. balsamifera* and *C. burmanni* leaves, compared with authentic standards of (−)- and (+)-borneol. Peak 1, (−)-borneol, peak 2, (+)-borneol. (B) Corresponding mass spectra of (−)- and (+)-borneol (upper halves), authentic standards of (−)- and (+)-borneol (lower halves). EIC, Extracted ion chromatograms.

centrifuged at 13,000×*g* for 10 min to separate the upper organic phase for analyzing by GC-MS (described previously [21]). The calibration curves for content determination are shown in Supplemental Fig. S1. All assays were performed in triplicate.

2.8. Fed-batch fermentation for (-)-borneol production

We use strain MD-B12 for fed-batch fermentation in a 5-L bioreactor (Shanghai Bailun Biotechnology Co., Ltd., China) to produce larger amounts of (-)-borneol. Firstly, a single clone was seeded into a 50 mL flask containing 10 mL of SD-Leu-Ura medium with 2.0% glucose and grown at 30 °C and 200 rpm for 48 h. The resulting exponential culture was diluted to an initial OD$_{600}$ of 0.3 in 200 mL of fresh SD-Leu-Ura medium and cultivated for another 12 h until the OD$_{600}$ reached approximately 5.0. Centrifuge the seed culture at 3000×*g*, resuspend it

Fig. 2. Partial alignment of BbTPS3 protein sequence with those of other known BPPSs. CbTPS1 (accession No. MW196671); SBS (accession No. AAC26017); LaBPPS (accession No. AJW68082); LdBPPS (accession No. ATY48638); AvBPPS (accession No. AWW87313). The conserved RRX$_8$W, DDXXD and NSE/DTE motifs are underlined.

with 50 mL of fresh SD-Leu-Ura medium, and inoculate into the bioreactor containing 1.9 L of SD-Leu-Ura medium with 2.0% glucose at an initial OD$_{600}$ of 0.3. The temperature was 30 °C and the pH was maintained at 5.0 by automatically adding 40% (v/v) NH$_3$·H$_2$O. Air flow was set at 1 vvm and the dissolved oxygen (DO) concentration was controlled above 40% saturation by agitation cascade (300–500 rpm). Concentrated 20 × optimized YP medium (OYP, 20% yeast extract, 40% peptone, 16% KH$_2$PO$_4$, and 12% MgSO$_4$) and 50% galactose was added into bioreactor after 24 h. An extraction phase comprising n-dodecane was added to 20% (v/v) of the medium volume after induced 6 h to start the two-phase extractive fermentation. 50% galactose was fed periodically into the fermentation to keep the galactose concentration under 1.0 g L^{-1}. Additionally, 20 × YP mixture (5% yeast extract, 15% peptone) was fed periodically to provide adequate nutrition for cell growth. At least independent duplicate samples were collected to determine the cell density, the (-)-borneol titer and GPP titer.

3. Results

3.1. Identification of the chirality of borneol in Blumea balsamifera and Cinnamomum burmanni leaves

The chirality and content of borneol in fresh leaves of *B. balsamifera* and *C. burmannii* were determined by GC-MS with a chiral column. After extracting the characteristic ion chromatograms of *m/z* 95, authentic standards of (-)-borneol (peak 1) and (+)-borneol (peak 2) were detected at retention times of 29.71 min and 30.02 min, respectively (Fig. 1A). Both peak 1 and peak 2 were detected in the leaves of *B. balsamifera* and *C. burmannii*. Peak 1 was significantly higher than peak 2 in *B. balsamifera*; in contrast, peak 2 was higher than peak 1 in *C. burmannii*. Next, we determined the contents of (+)- and (-)-borneol in plant leaves using a standard curve. Almost all of the borneol in *B. balsamifera* was (-)-borneol (4.80 ± 1.38 g kg^{-1}), accounting for
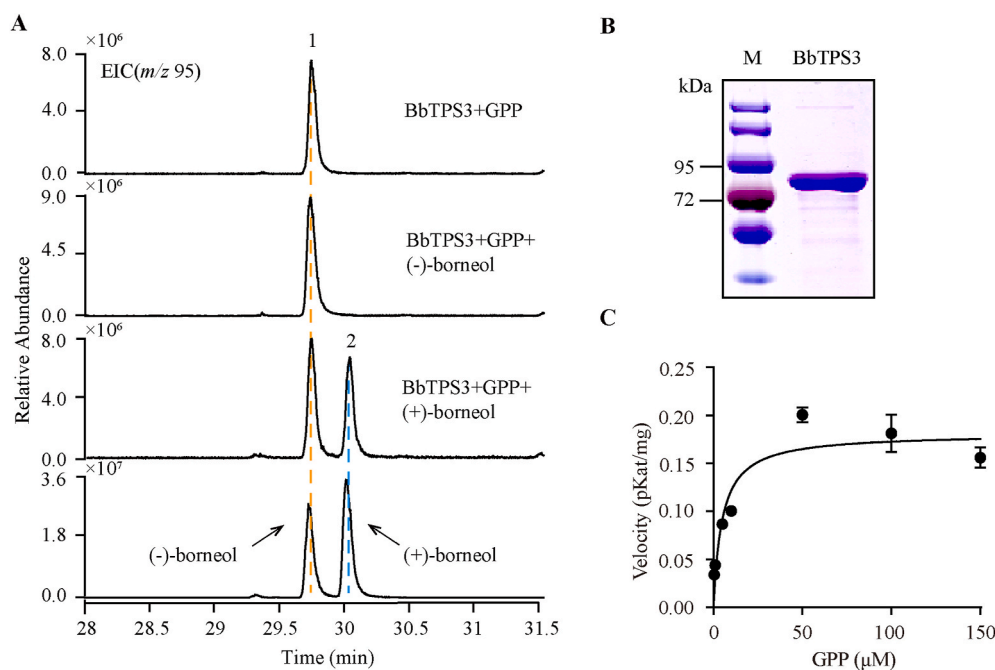
Fig. 3. GC-MS analysis of *in vitro* assays with BbTPS3. (A) Extracted ion chromatograms of *m/z* 95 *in vitro* assays with purified BbTPS3 and GPP as a substrate. Peak 1, (−)-borneol, Peak 2, (+)-borneol. (B) SDS-PAGE of BbTPS3 *in vitro* assays. (C) Velocity of BbTPS3 at increasing GPP concentrations. The data are averages of three biological replicates with error bars representing standard deviations.
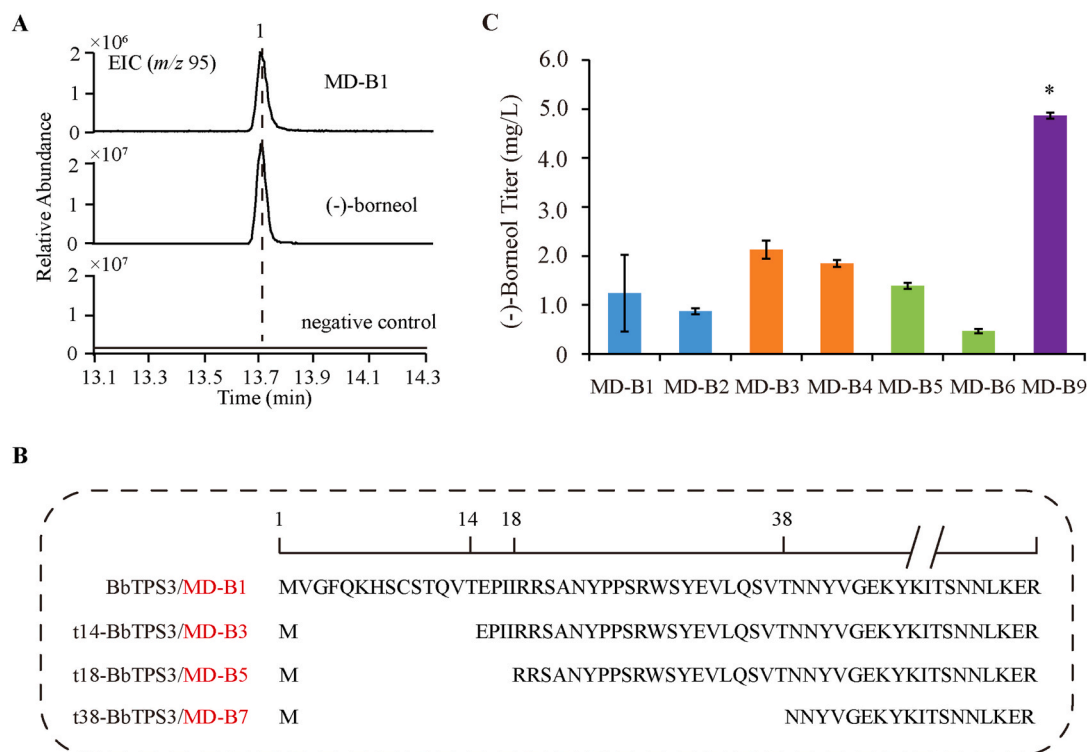
Fig. 4. The (−)-borneol production of strains expressing truncations and adding Kozak sequence of the BbTPS3. (A) Extracted ion chromatograms of *m/z* 95 of (−)-borneol production in CEN.PK2-1D (negative control) and the MD-B1 strain. (B) Schematic of the truncated position of N-terminus of BbTPS3. (C) The titer of (−)-borneol product in strains expressing the truncated and added Kozak sequence proteins. The data are averages of three biological replicates with error bars representing standard deviations. (*) represent means which are significantly different at $p < 0.05$.

99.40% of the total borneol in leaves. (+)-Borneol accounted for 94.95% of total borneol in *C. burmannii* leaves (3.79 ± 0.75 g kg^{-1}).

3.2. Transcriptome-based discovery of BbTPS3 in Blumea balsamifera

In our previous study, we identified a highly specific (+)-bornyl diphosphate synthase, CbTPS1, in *C. burmannii*, whose main product *in vitro* was (+)-borneol [10]. The fresh leaves of *B. balsamifera* containing large amounts of (-)-borneol were used to produce a transcriptome library, and then TPS candidates were screened by performing homology-based searches of the transcriptome. TRINITY_DN19922_c0_g2_i1 had the highest identity with the reported TPS genes. Specific primers were designed to clone the corresponding candidate gene from *B. balsamifera* cDNA, and the sequence was annotated as *BbTPS3*. *BbTPS3* has an open reading frame of 1671 bp and encodes a 556-residue enzyme with a molecular mass of 64.56 kDa. Plant terpene synthases are divided into seven different subfamilies, named TPS-a to TPS-g, according to amino acid sequence similarity [25]. BbTPS3 belongs to the TPS-b group, which mainly contains angiosperm monoterpene synthases. All members of the TPS-b clade, including BbTPS3, contain the highly conserved aspartate-rich motifs DDXXD and NSE/DTE, which take part in substrate binding and metal-dependent ionization, and the RRX$_8$W motif, which is responsible for monoterpenoid cyclization [26]. Comparison of amino acid sequences showed that BbTPS3 shared the highest identities with SBS (38.37%) from *S. officinalis* [15] (Fig. 2), followed by LaBPPS (37.21%) from *L. angustifolia* [16], LdBPPS (36.33%) from *L. dulcis* [16], CbTPS1 (36.16%) from *C. burmannii* [10], and AvBPPS from *A. villosum* (34.33%) [18].

3.3. Functional characterization of BbTPS3

In vitro activity was analyzed using GPP as a substrate. The purified

BbTPS3 protein generated borneol as its main product and other minor monoterpenoids (Fig. S4). No product formation was found in the absence of alkaline phosphatase, calf intestinal (CIAP) or when the empty vector was transformed into *E. coli* Transetta (DE3) cells. The chirality of borneol was investigated using a chiral column (Fig. 3A). One peak (peak 1) was the same as that of the authentic standard (-)-borneol. When the authentic standard (-)-borneol was added to the reaction product, the peak remained unchanged, but when the authentic standard (+)-borneol was added, one more peak (peak 2) was detected. This result confirmed that BbTPS3 catalyzed GPP to (-)-borneol in the presence of CIAP. Next, BbTPS3 was purified using Ni-NTA affinity column chromatography (Fig. 3B). Kinetic analysis demonstrated that BbTPS3 had a K_m value of 4.93 ± 1.38 μM for GPP, and the corresponding k_{cat} value was 1.49 s^{-1} (Fig. 3C).

3.4. Improving the (-)-borneol yield by generating tailored truncations

BbTPS3 was codon-optimized and introduced into the GPP high-yield strain MD, which harbors an optimized exogenous MVA pathway and was developed in our previous work [10]. (-)-Borneol was produced with a yield of 1.24 mg·L^{-1} in the resulting strain, MD-B1, and no product was found when the codon-optimized BbTPS3 was overexpressed in yeast strain CEN.PK2-1D (Fig. 4A). Plant TPS enzymes, including BbTPS3, have an N-terminal plastidic transit peptide that targets the protein to the plastid stroma and stromules where it is proteolyzed [27–29]. To increase the (-)-borneol titer, we overexpressed different N-terminal truncations of BbTPS3 overexpressed in yeast. Based on the ChloroP (http://www.cbs.dtu.dk/services/ChloroP/) predictions, BbTPS3 was truncated at three different positions (T14, I18, and T38) in the N-terminus; these truncated proteins were named t14-BbTPS3, t18-BbTPS3, and t38-BbTPS3, respectively. As illustrated in Fig. 4B, three (-)-borneol-producing strains were constructed and the titer of (-)-borneol in each strain was determined by GC-MS. Expression of the
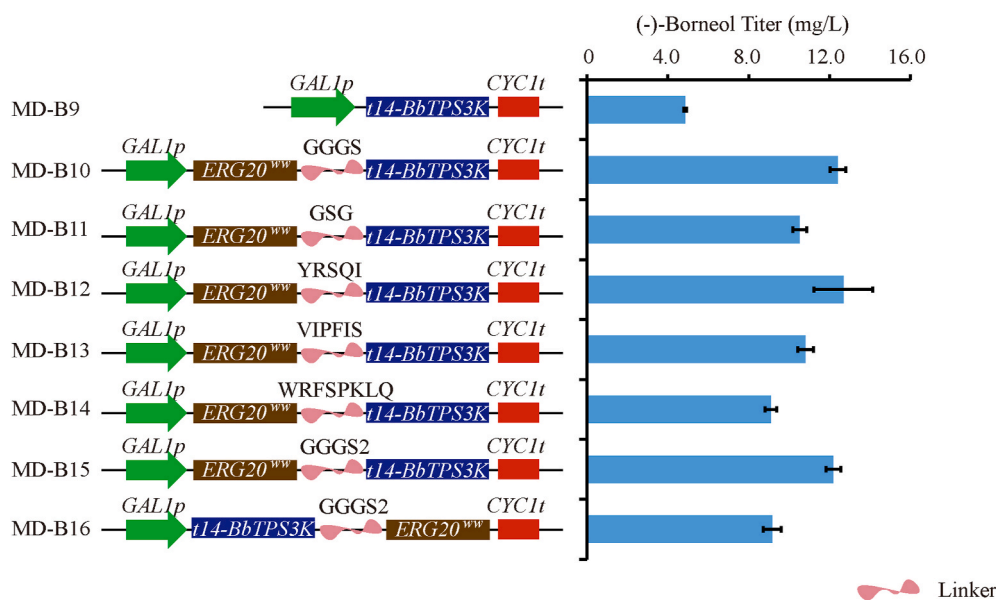
Fig. 5. The (−)-borneol production of strains expressing the fusion proteins. The data are averages of 3 biological replicates with error bars representing standard deviations.

truncated t14-BbTPS3 and t18-BbTPS3 proteins led to an increase in (-)-borneol production. Strain MD-B3 expressing t14-BbTPS3 produced 2.13 mg·L^{-1} of (-)-borneol, which was 1.72-fold higher than that amount produced by the strain MD-B1 (expressing full-length BbTPS3), and the strain MD-B5 expressing t18-BbTPS3 produced 1.12-fold higher levels of (-)-borneol (1.39 mg·L^{-1}) than the MD-B1 (Fig. 4C). However, no (-)-borneol was detected in strain MD-B7 expressing t38-BbTPS3 (data not shown).

3.5. Improving the (-)-borneol yield by adding a Kozak sequence

Highly expressed genes in *S. cerevisiae* seem to prefer a 5′-UTR rich in adenine and poor in guanine, particularly in the Kozak sequence that occupies roughly the first six nucleotides upstream of the START codon [22,24]. Thus, the Kozark sequence is used to improve gene expression here. The Kozak sequence "GCCACC" was added in front of the start codon (ATG) of the codon-optimized full-length and truncated BbTPS3 proteins to improve (-)-borneol production. The modified proteins were named BbTPS3K, t14-BbTPS3K, t18-BbTPS3K, and t38-BbTPS3K. However, when we introduced the modified proteins into the strain MD, there were no further improvements in (-)-borneol yield. As shown in Fig. 4C, the yields of strains expressing BbTPS3K, t14-BbTPS3K, t18-BbTPS3K, and t38-BbTPS3K were 0.87 mg·L^{-1} (strain MD-B2),

1.85 mg·L^{-1} (strain MD-B4), 0.47 mg·L^{-1} (strain MD-B6), and 0.00 mg·L^{-1} (strain MD-B8, data not shown), respectively. In yeast, "AAAAAA" is the specific Kozak sequence. Therefore, "AAAAAA" was used in place of "GCCACC" in front of the ATG of t14-BbTPS3, which had the highest (-)-borneol yield, generating the modified protein t14-BbTPS3K2. The introduction of t14-BbTPS3K2 into strain MD (strain MD-B9) significantly improved (-)-borneol production to 4.87 mg·L^{-1} (Fig. 4C).

3.6. Improving the (-)-borneol yield by constructing fusion proteins

Fusion proteins are generated by fusing two or more coding sequences separated by a linker region; this method has been the most widely used to enhance the catalytic activities of enzymes [30]. GPP, which is the precursor for various yeast essential metabolites, such as squalene and steroid, is encoded by the gene *ERG20* [31–33]. Therefore, we fused ERG20$^{F96W-N127W}$ with t14-BbTPS3K2 to improve (-)-borneol production. Previous studies indicated that the length of the flexible linker and the order of the proteins determine the amount of folding interference and whether the two fusion proteins fold correctly [34,35]. In this study, we examined five linkers of different lengths, "GGGS", "GSG", "YRSQI", "VIPFIS", and "WRFSPKLQ". We constructed five fusion proteins (ERG20$^{F96W-N127W}$-GGGS-t14-BbTPS3K2,
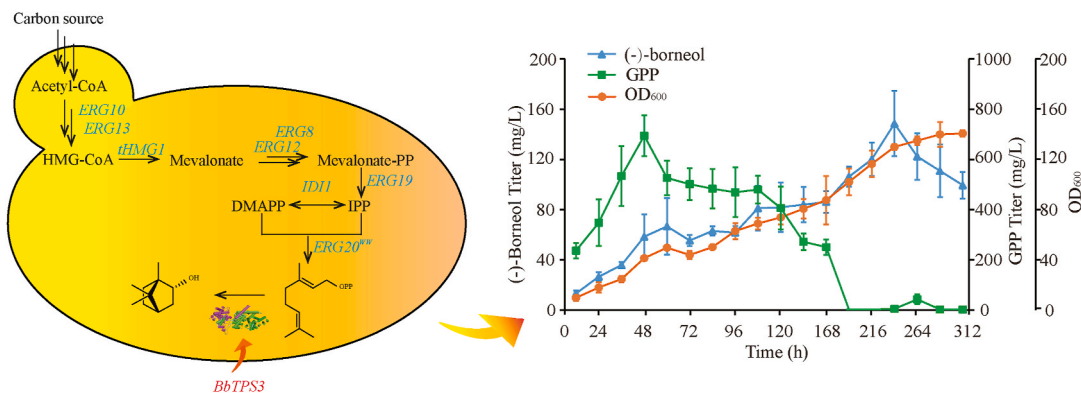
Fig. 6. Production of (−)-borneol in fed-batch fermentation using the engineered strain MD-B12 in a 5-L bioreactor. The data are averages of 3 biological replicates with error bars representing standard deviations.

ERG20$^{F96W-N127W}$-GSG-t14-BbTPS3K2, ERG20$^{F96W-N127W}$-YRSQI-t14-BbTPS3K2, ERG20$^{F96W-N127W}$-VIPFIS-t14-BbTPS3K2, and ERG20$^{F96W-N127W}$-WRFSPKLQ-t14-BbTPS3K2, Supplemental Fig. S5). ERG20$^{F96W-N127W}$-GGGS-t14-BbTPS3K2 was selected to investigate the impact of nucleotide sequence and order of the flexible linker. Then, another two fusion proteins, ERG20$^{F96W-N127W}$-GGGS-t14-BbTPS3K2-2 and t14-BbTPS3K2-GGGS-ERG20$^{F96W-N127W}$-2, were constructed to investigate the effect of protein order and nucleic acid sequence on activity.

The strains expressing the seven fusion proteins had higher (-)-borneol titers than the control strain MD-B9 (Fig. 5). Among these fusions, ERG20$^{F96W-N127W}$-YRSQI-t14-BbTPS3K2 (strain MD-B12) resulted in the highest yield of (-)-borneol (12.68 mg·L^{-1}), which was 10-fold higher compared with that of the strain MD-B1. The (-)-borneol yields of strains expressing ERG20$^{F96W-N127W}$-GGGS-t14-BbTPS3K2 (strain MD-B10), ERG20$^{F96W-N127W}$-GSG-t14-BbTPS3K2 (strain MD-B11), ERG20$^{F96W-N127W}$-VIPFIS-t14-BbTPS3K2 (strain MD-B13), and ERG20$^{F96W-N127W}$-GGGS-t14-BbTPS3K2 (strain MD-B15) were 12.41 mg·L^{-1}, 10.52 mg·L^{-1}, 10.81 mg·L^{-1}, and 12.19 mg·L^{-1}, respectively. The levels of (-)-borneol produced by strains expressing ERG20$^{F96W-N127W}$-WRFSPKLQ-t14-BbTPS3K2 (strain MD-B14) and t14-BbTPS3K2-GGGS-ERG20$^{F96W-N127W}$-2 (strain MD-B16) were 9.10 mg·L^{-1} and 9.16 mg·L^{-1}, respectively; these levels were 7-fold higher than those produced by strain MD-B1.

3.7. Achieving high titers of (-)-borneol by fed-batch fermentation

To further increase the titer of (-)-borneol, the best strain, MD-B12, was used for the production of (-)-borneol in fed-batch fermentation. SD-Leu-Ura medium was used to promote plasmid retention. The strains were inoculated into a 5-L bioreactor to an initial OD$_{600}$ of 0.3. After culturing for 24 h, the medium was replaced with OYP. As shown in Fig. 6, the total titer of (-)-borneol reached almost 148.59 mg·L^{-1}, which is the highest titer of (-)-borneol titer reported for *S. cerevisiae*. The biomass of the strains increased rapidly before 60 h, and growth gradually increased until a maximum OD$_{600}$ of 140.70 was reached at 312 h. The titer of (-)-borneol was significantly positively correlated with biomass. (-)-Borneol continued to accumulate until 240 h, reaching a titer of 148.59 mg·L^{-1}. Thereafter the yield declined, but the biomass remained stable. By contrast, GPP accumulated rapidly with increasing biomass during the first 48 h, but it decreased with the accumulation of (-)-borneol. Only trace amounts GPP were detected at the end of the fermentation.

4. Discussion

Borneol is a rare and precious natural product that is widely used in the medicine, perfume, and chemical industries because of its unique aroma; therefore, it is referred to as soft gold. Borneol is a dicyclic monoterpenoid with two chiral structures, (-)-borneol and (+)-borneol. Both have similar properties and have anti-inflammatory and analgesic effects. The synthesis of (+)-borneol has been well studied, but that of (-)-borneol has rarely been investigated. Here, the chirality of borneol in *B. balsamifera* was characterized for the first time, and the results indicated that (-)-borneol is the predominant form of borneol in *B. balsamifera*, accounting for 99.40% of the total borneol in leaves. We then identified a high-efficiency BbTPS3 from *B. balsamifera* that reacts with GPP to produce (-)-borneol *in vitro* in the presence of CIAP. Although several (+)-bornyl diphosphate synthases have been reported in plants, BbTPS3 is the first reported (-)-bornyl diphosphate synthase. The K_m value of BbTPS3 (4.93 ± 1.38 μM) for GPP is similar to that of CbTPS1 (5.11 μM) and SBS (3.0 μM) but lower than that of other reported monoterpene synthases (13.10–26.12 μM), indicating that BbTPS3 has a higher affinity for GPP than most monoterpene synthases [15,36–38]. Thus, this gene will be useful in efforts to reconstruct the (-)-borneol biosynthetic pathway for heterologous production.

GPP is the direct precursor of monoterpenoids [8]. We selected the

yeast strain MD, which was engineered to produce high levels of GPP [10]. Then, multiple strategies were applied to increase the production of (-)-borneol. The codon-optimized BbTPS3 was first truncated at the N-terminus and a Kozak sequence was placed in front of the ATG. The highest (-)-borneol titer was achieved in strain MD-B9, which expresses the modified protein t14-BbTPS3K2. The titer (4.87 mg·L^{-1}) was 4-fold higher than that of strain MD-B1. Next, five linkers with different lengths and protein orders were tested. The strain MD-B12 expressing the fusion module ERG20$^{F96W-N127W}$-YRSQI-t14-BbTPS3K2 produced 12.68 mg·L^{-1} (-)-borneol. Therefore, a combination of truncation, Kozak sequence addition, and fusion protein construction is an effective strategy for improving (-)-borneol production. This strain produced a titer of (-)-borneol 148.59 mg·L^{-1} in a 5-L bioreactor, which is the highest (-)-borneol titer achieved in heterologous production reported so far.

Though more than 100 mg·L^{-1} of (-)-borneol was produced in this study, the yield is still well below the level required for industrial applications and that achieved for other terpenoids [8,39,40], such as artemisinic acid (25 g L^{-1}) [41]. The efficiency of generating the final product is affected by many factors. Monoterpenes, such as linalool and borneol, alter membrane properties or damage the cell wall and are highly toxic to *S. cerevisiae*, reducing the production efficiency [42,43]. Here, we used two-phase extractive fermentation to reduce toxicity. It was recently reported that transformation of yeast peroxisomes into microfactories for monoterpenoid production can achieve up to a 125-fold increase over cytosolic production by reducing cytotoxicity [38,44]. Multiple engineering strategies can be applied to optimize the metabolic pathway of host cells and increase the supply of GPP [11,45]. In addition, directed evolution of enzymes and optimization of the fermentation strategy will further enhance production [46,47]. Our work lays a solid foundation for the biosynthesis of natural (-)-borneol and other active pharmaceutical terpenoids.

Declaration of competing interest

The authors declare no conflict of interest.

CRediT authorship contribution statement

Rui Ma: Conceptualization, Methodology, Writing – original draft, Writing – review & editing. **Ping Su:** Conceptualization, Methodology, Investigation, Writing – original draft. **Qing Ma:** Methodology, Supervision. **Juan Guo:** Formal analysis. **Suiqing Chen:** Investigation. **Baolong Jin:** Data curation. **Haiyan Zhang:** Resources. **Jinfu Tang:** Software. **Tao Zhou:** Funding acquisition. **Chenghong Xiao:** Funding acquisition. **Guanghong Cui:** Supervision, Project administration. **Luqi Huang:** Supervision, Project administration.

Declaration of competing interest

The authors declare that they have no known competing financial interests or personal relationships that could have appeared to influence the work reported in this paper.

Acknowledgements

Appendix A. Supplementary data

Supplementary data to this article can be found online at https://doi.org/10.1016/j.synbio.2021.12.004.

References

[1] Bhatia SP, Letizia CS, Api AM. Fragrance material review on borneol. Food Chem Toxicol 2008;46:77–80. https://doi.org/10.1016/j.fct.2008.06.031.

[2] Zielińska-Błajet M, Feder-Kubis J. Monoterpenes and their derivatives—recent development in biological and medical applications. Int J Mol Sci 2020;21:1–38. https://doi.org/10.3390/ijms21197078.

[3] Vohra S, Musgaard M, Bell SG, Wong LL, Zhou W, Biggin PC. The dynamics of camphor in the cytochrome P450 CYP101D2. Protein Sci 2013;22:1218–29. https://doi.org/10.1002/pro.2309.

[4] Chen W, Vermaak I, Viljoen A. Camphor-A fumigant during the black death and a coveted fragrant wood in ancient Egypt and babylon-A review. Molecules 2013;18: 5434–54. https://doi.org/10.3390/molecules18055434.

[5] Ma R, Xie Q, Li H, Guo X, Wang J, Li Y, et al. l-Borneol exerted the neuroprotective effect by promoting Angiogenesis coupled with neurogenesis via Ang1-VEGF-BDNF pathway. Front Pharmacol 2021;12:1–17. https://doi.org/10.3389/fphar.2021.641894.

[6] Vasconcelos RMC, Leite FC, Leite JA, Rodrigues Mascarenhas S, Rodrigues LC, Piuvezam MR. Synthesis, acute toxicity and anti-inflammatory effect of bornyl salicylate, a salicylic acid derivative. Immunopharmacol Immunotoxicol 2012;34: 1028–38. https://doi.org/10.3109/08923973.2012.694891.

[7] Sokolova AS, Yarovaya OI, Shtro AA, Borisova MS, Morozova EA, Tolstikova TG, et al. Synthesis and biological activity of heterocyclic borneol derivatives. Chem Heterocycl Compd 2017;53:371–7. https://doi.org/10.1007/s10593-017-2063-3.

[8] Jiang GZ, Yao MD, Wang Y, Zhou L, Song TQ, Liu H, et al. Manipulation of GES and ERG20 for geraniol overproduction in Saccharomyces cerevisiae. Metab Eng 2017; 41:57–66. https://doi.org/10.1016/j.ymben.2017.03.005.

[9] Zhou L, Wang Y, Han L, Wang Q, Liu H, Cheng P, et al. Enhancement of patchoulol production in Escherichia coli via multiple engineering strategies. J Agric Food Chem 2021;69:7572–80. https://doi.org/10.1021/acs.jafc.1c02399.

[10] Ma R, Su P, Guo J, Jin B, Ma Q, Zhang H, et al. Bornyl diphosphate synthase from Cinnamomum burmanni and its application for (+)-Borneol biosynthesis in yeast. Front Bioeng Biotechnol 2021;9:1–11. https://doi.org/10.3389/fbioe.2021.631863.

[11] Lei D, Qiu Z, Wu J, Qiao B, Qiao J, Zhao GR. Combining metabolic and monoterpene synthase engineering for de Novo production of monoterpene alcohols in Escherichia coli. ACS Synth Biol 2021;10:1531–44. https://doi.org/10.1021/acssynbio.1c00081.

[12] Cao X, Wei LJ, Lin JY, Hua Q. Enhancing linalool production by engineering oleaginous yeast Yarrowia lipolytica. Bioresour Technol 2017;245:1641–4. https://doi.org/10.1016/j.biortech.2017.06.105.

[13] Cao X, Lv YB, Chen J, Imanaka T, Wei LJ, Hua Q. Metabolic engineering of oleaginous yeast Yarrowia lipolytica for limonene overproduction. Biotechnol Biofuels 2016;9:1–11. https://doi.org/10.1186/s13068-016-0626-7.

[14] Laule O, Fürholz A, Chang HS, Zhu T, Wang X, Heifetz PB, et al. Crosstalk between cytosolic and plastidial pathways of isoprenoid biosynthesis in Arabidopsis thaliana. Proc Natl Acad Sci U S A 2003;100:6866–71. https://doi.org/10.1073/pnas.1031755100.

[15] Wise ML, Savage TJ, Katahira E, Croteau R. Monoterpene synthases from common sage (Salvia officinalis). J Biol Chem 1998;273:14891–9. https://doi.org/10.1074/jbc.273.24.14891.

[16] Despinasse Y, Fiorucci S, Antonczak S, Moja S, Bony A, Nicolè F, et al. Bornyl-diphosphate synthase from Lavandula angustifolia: a major monoterpene synthase involved in essential oil quality. Phytochemistry 2017;137:24–33. https://doi.org/10.1016/j.phytochem.2017.01.015.

[17] Hurd MC, Kwon M, Ro DK. Functional identification of a Lippia dulcis bornyl diphosphate synthase that contains a duplicated, inhibitory arginine-rich motif. Biochem Biophys Res Commun 2017;490:963–8. https://doi.org/10.1016/j.bbrc.2017.06.147.

[18] Wang H, Ma D, Yang J, Deng K, Li M, Ji X, et al. An integrative volatile terpenoid profiling and transcriptomics analysis for gene mining and functional characterization of avbpps and avps involved in the monoterpenoid biosynthesis in amomum villosum. Front Plant Sci 2018;9:1–16. https://doi.org/10.3389/fpls.2018.00846.

[19] Yang Z, An W, Liu S, Huang Y, Xie C, Huang S, et al. Mining of candidate genes involved in the biosynthesis of dextrorotatory borneol in Cinnamomum burmannii by transcriptomic analysis on three chemotypes. PeerJ 2020;2020. https://doi.org/10.7717/peerj.9311.

[20] Su P, Guan H, Zhao Y, Tong Y, Xu M, Zhang Y, et al. Identification and functional characterization of diterpene synthases for triptolide biosynthesis from Tripterygium wilfordii. Plant J 2018;93:50–65. https://doi.org/10.1111/tpj.13756.

[21] Ma R, Su P, Jin B, Guo J, Tian M, Mao L, et al. Molecular cloning and functional identification of a high-efficiency (+)-borneol dehydrogenase from Cinnamomum camphora (L.) Presl. Plant Physiol Biochem 2020. https://doi.org/10.1016/j.plaphy.2020.11.023.

[22] Li J, Liang Q, Song W, Marchisio MA. Nucleotides upstream of the Kozak sequence strongly influence gene expression in the yeast S. cerevisiae. J Biol Eng 2017;11: 1–14. https://doi.org/10.1186/s13036-017-0068-1.

[23] Hernández G, Osnaya VG, Pérez-Martínez X. Conservation and variability of the AUG initiation codon context in eukaryotes. Trends Biochem Sci 2019;44:1009–21. https://doi.org/10.1016/j.tibs.2019.07.001.

[24] Hamilton R, Watanabe CK, Boer De HA. Compilation and comparison of the s ce context around the AUG startcodons in Saccharomyces cemisiae. mRNAs 1987;15: 3581–93. https://doi.org/10.1093/nar/15.8.3581.

[25] Zhou F, Pichersky E. The complete functional characterisation of the terpene synthase family in tomato. New Phytol 2020;226:1341–60. https://doi.org/10.1111/nph.16431.

[26] Chen F, Tholl D, Bohlmann J, Pichersky E. The family of terpene synthases in plants: a mid-size family of genes for specialized metabolism that is highly diversified throughout the kingdom. Plant J 2011;66:212–29. https://doi.org/10.1111/j.1365-313X.2011.04520.x.

[27] Rowland E, Kim J, Bhuiyan NH, Van Wijk KJ. The arabidopsis chloroplast stromal n-terminome: complexities of amino-terminal protein maturation and stability. Plant Physiol 2015;169:1881–96. https://doi.org/10.1104/pp.15.01214.

[28] Zybailov B, Rutschow H, Friso G, Rudella A, Emanuelsson O, Sun Q, et al. Sorting signals, N-terminal modifications and abundance of the chloroplast proteome. PLoS One 2008;3. https://doi.org/10.1371/journal.pone.0001994.

[29] Bohlmann J, Meyer-Gauen G, Croteau R. Plant terpenoid synthases: molecular biology and phylogenetic analysis. Proc Natl Acad Sci U S A 1998;95:4126–33. https://doi.org/10.1073/pnas.95.8.4126.

[30] Woolston BM, Edgar S, Stephanopoulos G. Metabolic engineering: past and future. Annu Rev Chem Biomol Eng 2013;4:259–88. https://doi.org/10.1146/annurev-chembioeng-061312-103312.

[31] Fischer MJC, Meyer S, Claudel P, Bergdoll M, Karst F. Metabolic engineering of monoterpene synthesis in yeast. Biotechnol Bioeng 2011;108:1883–92. https://doi.org/10.1002/bit.23129.

[32] Siddiqui MS, Thodey K, Trenchard I, Smolke CD. Advancing secondary metabolite biosynthesis in yeast with synthetic biology tools. FEMS Yeast Res 2012;12: 144–70. https://doi.org/10.1111/j.1567-1364.2011.00774.x.

[33] Karst F, Plochocka D, Meyer S, Szkopinska A. Farnesyl diphosphate synthase activity affects ergosterol level and proliferation of yeast Saccharomyces cerevisae. Cell Biol Int 2004;28:193–7. https://doi.org/10.1016/j.cellbi.2003.12.001.

[34] Tanaka E, Mizumori Y, Komatsu C, Ando W. Realizing the safe society/products and services: social network service extension of WebryBlog. NEC Tech J 2006;1: 120–2. https://doi.org/10.1016/j.addr.2012.09.039.Fusion.

[35] Reddy Chichili VP, Kumar V, Sivaraman J. Linkers in the structural biology of protein-protein interactions. Protein Sci 2013;22:153–67. https://doi.org/10.1002/pro.2206.

[36] Ignea C, Raadam MH, Motawia MS, Makris AM, Vickers CE, Kampranis SC. Orthogonal monoterpenoid biosynthesis in yeast constructed on an isomeric substrate. Nat Commun 2019;10:1–15. https://doi.org/10.1038/s41467-019-11290-x.

[37] Morehouse BR, Kumar RP, Matos JO, Olsen SN, Oprian DD. Functional and structural characterization of a (+)-Limonene synthase from citrus sinensis. Biochemistry 2017;56:1706–15. https://doi.org/10.1021/acs.biochem.7b00143.

[38] Dusséaux S, Wajn WT, Liu Y, Ignea C, Kampranis SC. Transforming yeast peroxisomes into microfactories for the efficient production of high-value isoprenoids. Proc Natl Acad Sci U S A 2020;117:31789–99. https://doi.org/10.1073/pnas.2013968117.

[39] Zhao J, Bao X, Li C, Shen Y, Hou J. Improving monoterpene geraniol production through geranyl diphosphate synthesis regulation in Saccharomyces cerevisiae. Appl Microbiol Biotechnol 2016;100:4561–71. https://doi.org/10.1007/s00253-016-7375-1.

[40] Zebec Z, Wilkes J, Jervis AJ, Scrutton NS, Takano E, Breitling R. Towards synthesis of monoterpenes and derivatives using synthetic biology. Curr Opin Chem Biol 2016;34:37–43. https://doi.org/10.1016/j.cbpa.2016.06.002.

[41] Paddon CJ, Westfall PJ, Pitera DJ, Benjamin K, Fisher K, McPhee D, et al. High-level semi-synthetic production of the potent antimalarial artemisinin. Nature 2013;496:528–32. https://doi.org/10.1038/nature12051.

[42] Demissie ZA, Tarnowycz M, Adal AM, Sarker LS, Mahmoud SS. A lavender ABC transporter confers resistance to monoterpene toxicity in yeast. Planta 2019;249: 139–44. https://doi.org/10.1007/s00425-018-3064-x.

[43] Brennan TCR, Krömer JO, Nielsen LK. Physiological and transcriptional responses of Saccharomyces cerevisiae to d-limonene show changes to the cell wall but not to the plasma membrane. Appl Environ Microbiol 2013;79:3590–600. https://doi.org/10.1128/AEM.00463-13.

[44] Zhou YJ, Buijs NA, Zhu Z, Gómez DO, Boonsombuti A, Siewers V, et al. Harnessing yeast peroxisomes for biosynthesis of fatty-acid-derived biofuels and chemicals with relieved side-pathway competition. J Am Chem Soc 2016;138:15368–77. https://doi.org/10.1021/jacs.6b07394.

[45] Ignea C, Raadam MH, Motawia MS, Makris AM, Vickers CE, Kampranis SC. Orthogonal monoterpenoid biosynthesis in yeast constructed on an isomeric substrate. Nat Commun 2019;10:3799. https://doi.org/10.1038/s41467-019-11290-x.

[46] Zhou J, Hu T, Gao L, Su P, Zhang Y, Zhao Y, et al. Friedelane-type triterpene cyclase in celastrol biosynthesis from Tripterygium wilfordii and its application for triterpenes biosynthesis in yeast. New Phytol 2019;223:722–35. https://doi.org/10.1111/nph.15809.

[47] Qu G, Li A, Acevedo-Rocha CG, Sun Z, Reetz MT. The crucial role of methodology development in directed evolution of selective enzymes. Angew Chem 2019. https://doi.org/10.1002/anie.201901491.